Monthly Notices
of the
ROYAL ASTRONOMICAL SOCIETY

Mon. Not. R. Astron. Soc. **420,** 658–671 (2012) doi:10.1111/j.1365-2966.2011.20080.x

Modelling pulsar glitches with realistic pinning forces: a hydrodynamical approach

B. Haskell,[1,2⋆] P. M. Pizzochero[3,4] and T. Sidery[5,6]

[1]*School of Mathematics, University of Southampton, Southampton SO17 1BJ*
[2]*Astronomical Institute 'Anton Pannekoek', University of Amsterdam, Science Park 904, 1098 XH Amsterdam, the Netherlands*
[3]*Dipartimento di Fisica, Università degli Studi di Milano, Via Celoria 16, 20133 Milano, Italy*
[4]*Istituto Nazionale di Fisica Nucleare, Sezione di Milano, Via Celoria 16, 20133 Milano, Italy*
[5]*FENS, Sabanci University, Orhanli, 34956 Istanbul, Turkey*
[6]*School of Physics and Astronomy, University of Birmingham, Edgbaston, Birmingham B15 2TT*

Accepted 2011 October 25. Received 2011 October 6; in original form 2011 July 26

ABSTRACT

Although pulsars are some of the most stable clocks in the Universe, many of them are observed to 'glitch', i.e. to suddenly increase their spin frequency ν with fractional increases that range from $\Delta\nu/\nu \approx 10^{-11}$ to 10^{-5}. In this paper, we focus on the 'giant' glitches, i.e. glitches with fractional increases in the spin rate of the order of $\Delta\nu/\nu \approx 10^{-6}$, that are observed in a subclass of pulsars including the Vela. We show that giant glitches can be modelled with a two-fluid hydrodynamical approach. The model is based on the formalism for superfluid neutron stars of Andersson & Comer and on the realistic pinning forces of Grill & Pizzochero. We show that all stages of Vela glitches, from the rise to the post-glitch relaxation, can be reproduced with a set of physically reasonable parameters and that the sizes and waiting times between giant glitches in other pulsars are also consistent with our model.

Key words: stars: neutron – pulsars: general – pulsars: individual: PSR B0833–45.

1 INTRODUCTION

The timing of radio pulsars provides us with one of the most stable clocks in the universe. Many pulsars exhibit, however, sudden increases in the spin rate, known as 'glitches'. To date, there have been glitches reported in more than 100 pulsars[1] (Melatos et al. 2008; Espinoza et al. 2011), with fractional jumps in the spin rate of $\Delta\nu/\nu \approx 10^{-11}$ to 10^{-5}.

There is still no clear consensus on the origin of these phenomena, but it is thought that glitches (at least the giant glitches that are observed in somewhat older, colder pulsars such as the Vela) are due to angular momentum being stored in a superfluid component of the star that is temporarily decoupled from the charged component to which the electromagnetic emission is anchored. When the two components recouple, there is a sudden transfer of angular momentum to the crust, which gives rise to the observed spin-up (Anderson & Itoh 1975). A superfluid rotates by forming a quantized array of vortices, the distribution of which determines the rotational profile of the star. The main idea at the base of most glitch models is that vortices can *pin* to the crustal lattice (Anderson & Itoh 1975; Alpar 1977; Pines et al. 1980; Alpar et al. 1981; Anderson et al. 1982), allowing a lag to build up between the superfluid and the charged component.

Following the seminal work of Baym, Pethick & Pines (1969), several models have been developed to explain the dynamical evolution of the pinned superfluid coupled to the crust, mainly with the intent of explaining the observed time-scales of days to months in the post-glitch recovery of the Vela pulsar. Essentially, one can distinguish two classes of models, those that assume that the relaxation is due to the weak coupling between the superfluid and the crust due to the interaction between free vortices and the coulomb lattice of nuclei (Jones 1990, 1992, 1998a) and those which rely on the creep model based on the seminal work of Alpar et al. (1984a) and later adaptations (Alpar et al. 1984b; Link, Epstein & Baym 1993; Larson & Link 2002). In this case, the assumption is that as a lag develops between the crust and the superfluid, vortices *creep* through the crust at a rate that is highly temperature-dependent, gradually transferring angular momentum and leading to a steady-state spin-down. However, when the lag approaches a critical value, it is possible for an instability to trigger a catastrophic unpinning event associated with a sudden transfer of angular momentum to the crust, after which vortices repin and a new equilibrium is reached. These models work remarkably well in explaining the post-glitch relaxation, but struggle to explain the exact nature of the perturbation which triggers it. Such an event may be triggered by large temperature perturbations (Link & Epstein 1996), caused for example by starquakes (Baym & Pines 1971; Cheng et al. 1992), the

⋆E-mail: b.d.l.haskell@uva.nl
[1] http://www.jb.man.ac.uk/pulsar/glitches/gTable.html

interactions of the proton vortices and the crustal magnetic field (Sedrakian & Cordes 1999) or, in the presence of strong crustal pinning, a two-stream instability in the superfluid flow may develop, leading to a sudden transfer of angular momentum (Glampedakis & Andersson 2009). Recently, however, Warszawski & Melatos (2011) have shown that glitches can be triggered by unpinning avalanches of the vortex array, leading to very promising results for the overall glitch size and waiting time distributions (see also Melatos & Warszawski 2009; Warszawski & Melatos 2010).

An entirely different mechanism was proposed by Ruderman (1991), who suggested that vortices pinned to the crust stress it to the point of fracture and then move outwards with the matter they are pinned to. Several other 'starquake' models have been proposed (Epstein & Link 2000; Franco, Link & Epstein 2000), but they are all based on the main assumption that a starquake triggers the outward motion of vortices pinned to the matter and the local rearrangement of the crust then causes an increase of the angle between the rotation axis and the magnetic axis, leading to an increased electromagnetic braking torque on the star. Note that starquakes had been invoked as a possible explanation for pulsar glitches very soon after the first observations, but had been ruled out as they could not account for the giant glitches of the Vela (Baym & Pines 1971; Ruderman 1975). This mechanism may, however, play a role in other systems, and in fact there is some evidence that smaller glitches in younger and hotter pulsars such as the Crab may be linked to starquakes (Middleditch et al. 2006). Furthermore, it has been suggested that the glitch may not be exclusively linked to vortex dynamics in the crust, but that the interaction between the vortices and the superconducting flux tubes in the core may contribute to the event (Ruderman, Zhu & Chen 1998; Sidery & Alpar 2009).

One of the main difficulties in constructing a glitch model is, however, the relative lack of realistic calculations for the pinning forces. Several calculations exist of the pinning *energy* and of the force per pinning site (Alpar 1977; Alpar et al. 1984a; Epstein & Baym 1988; Link & Epstein 1991; Pizzochero, Viverit & Broglia 1997; Jones 1998b; Donati & Pizzochero 2003, 2004, 2006; Avogadro et al. 2007), but such calculations of the pinning force neglect the finite length of the vortices and rely on simplified geometries. Recently, however, Link (2009) has analysed the motion of a vortex in a random potential and, even more crucially, Grill & Pizzochero (in preparation) have obtained realistic estimates of the pinning force *per unit length* of the vortex, the quantity that can be directly compared to the Magnus force which tends to push the vortices out and force the superfluid into corotation with the crust.

Pizzochero (2011) has recently shown that a simple analytic model, based on the catastrophic unpinning paradigm and the realistic pinning forces calculated by Grill & Pizzochero (in preparation) (see also Grill 2011), can describe glitches in the 'Vela'-like pulsars, which are typically older, exhibit larger glitches ($\Delta\nu/\nu \approx 10^{-7}$ to 10^{-6}) and always show a decrease in the frequency derivative after the glitch (Espinoza et al. 2011). Essentially, the assumption is that as the star spins down, the vorticity is accumulated in the strong pinning region and then released once the resulting Magnus force exceeds the maximum of the pinning force.

In order to make quantitative predictions for the observed jump in frequency and subsequent relaxation of the crust, it is, however, also necessary to describe the evolution of the various fluid components that form the neutron star (NS). In order to do this, it is convenient to follow a hydrodynamical approach that does not deal with vortex motion directly, but rather follows the evolution of the separate fluid components. In particular, we shall make use of the multifluid formalism developed by Andersson & Comer (2006) and recently applied, albeit in a much simpler formulation, to the study of pulsar glitches by Sidery et al. (2010). In the following, we shall thus go beyond the analytic model of Pizzochero (2011) and show how the realistic pinning results of Grill & Pizzochero (in preparation) can be incorporated into this formalism and used to accurately reproduce, for a reasonable range of parameters, the observed properties of pulsar glitches. Furthermore, as we will discuss in the following sections, we will assume that the relaxation is entirely due to the mutual friction between the superfluid component and the 'normal' fluid. In a sense, we are thus taking the view of Jones (1992) that the relaxation is due to the dynamics of vortices close to corotation with the superfluid, rather than to vortex 'creep'. Note, however, that the creep model has been shown to be consistent with the observed relaxation time-scales of the Vela pulsar in the linear regime (Alpar, Cheng & Pines 1989), and we can thus qualitatively account for it by rescaling the mutual friction parameters, as will be discussed in the following. Finally, let us also point out that an effect that is neglected in this preliminary model is that of Ekman pumping at the crust–core interface, which has been shown, together with shear viscosity, to be relevant in explaining the post-glitch relaxation times (van Eysden & Melatos 2010) and should be included in future developments.

Let us stress that such detailed theoretical work is crucial at this time, as the new Low Frequency Array (LOFAR) radio telescope has just come online and begun observations of pulsars and fast radio transients (Stappers et al. 2011). As development continues, LOFAR and in the future the Square Kilometre Array (SKA) are likely to not only provide a wealth of data on both known and new glitching pulsars, but also resolve (or at least tightly constrain) the glitch rise time, thus allowing us to test our theoretical understanding of the glitch mechanism (Smits et al. 2009). Furthermore, a glitch may trigger a gravitational wave (GW) burst which could be detectable by next generation GW observatories (Bennett, van Eysden & Melatos 2010; Sidery et al. 2010). By accurately determining the glitch time, LOFAR and the SKA could be used to trigger a directed GW search.

Finally, the constructions of long-term hydrodynamical simulations of NS interior could also be extended to model not only large pulsar glitches, but more generally pulsar timing noise, in order to understand the role that the interior dynamics of the star plays compared to magnetospheric processes, which have been shown to be at work in some systems (Lyne et al. 2010). This is an issue that is of great importance for the current efforts to detect GWs with pulsar timing arrays (Hobbs et al. 2010).

2 TWO-FLUID EQUATIONS OF MOTION

We model the pulsar as a two-fluid system of superfluid neutrons and a charged component, which consists of the crust and the charged particles in the interior. As the neutrons are superfluid, they will rotate by forming an array of quantized vortices, the interaction of which with the fluids will give rise to a weak coupling between the components, known as mutual friction. To describe the equations of motion of the crust and of the superfluid, we shall use the two-fluid formalism for NS cores developed by Andersson & Comer (2006). We thus do not consider the equations of motion of the vortices, but rather model the macroscopic motion of two dynamical degrees of freedom, representing the superfluid neutrons and a neutral conglomerate of protons, electrons and all non-superfluid components that are strongly coupled to them. Assuming that the individual

species are conserved, we have the standard conservation laws,

$$\partial_t \rho_x + \nabla_i \left(\rho_x v_x^i\right) = 0, \tag{1}$$

where the constituent index x may be either p or n. The Euler equations take the form

$$\left(\partial_t + v_x^j \nabla_j\right)\left(v_i^x + \varepsilon_x w_i^{yx}\right) + \nabla_i(\tilde{\mu}_x + \Phi) + \varepsilon_x w_{yx}^j \nabla_i v_j^x = f_i^x/\rho_x, \tag{2}$$

where $w_i^{yx} = v_i^y - v_i^x$ $(y \neq x)$ and $\tilde{\mu}_x = \mu_x/m_x$ represents the chemical potential (in the following, we assume that $m_\mathrm{p} = m_\mathrm{n}$). Moreover, Φ represents the gravitational potential, and the parameter ε_x encodes the entrainment effect. The force on the right-hand side of (2) can be used to describe other interactions, including dissipative terms (Andersson & Comer 2006). We will focus on the vortex-mediated mutual friction force. This means that we consider a force of the form (Andersson, Sidery & Comer 2006)

$$f_i^x = \kappa n_\mathrm{v} \rho_\mathrm{n} \mathcal{B}' \epsilon_{ijk} \hat{\Omega}_\mathrm{n}^j w_{xy}^k + \kappa n_\mathrm{v} \rho_\mathrm{n} \mathcal{B} \epsilon_{ijk} \hat{\Omega}_\mathrm{n}^j \epsilon^{klm} \hat{\Omega}_l^\mathrm{n} w_m^{xy}, \tag{3}$$

where Ω^j is the angular frequency of the neutron fluid (a hat represents a unit vector), $\kappa = h/2m_\mathrm{n}$ represents the quantum of circulation and n_v is the vortex number per unit area. In particular, the quantity κn_v is linked to the rotation rate of the neutrons and protons by the relation (where $\tilde{r}$ is the cylindrical radius)

$$\kappa n_\mathrm{v} = 2\left[\Omega_\mathrm{n} + \varepsilon_\mathrm{n}(\Omega_\mathrm{p} - \Omega_\mathrm{n})\right] + \tilde{r}\frac{\partial}{\partial \tilde{r}}\left[\Omega_\mathrm{n} + \varepsilon_\mathrm{n}(\Omega_\mathrm{p} - \Omega_\mathrm{n})\right]. \tag{4}$$

One can express the mutual friction force in terms of a dimensionless 'drag' parameter $\mathcal{R}$ such that (Andersson et al. 2006)

$$\mathcal{B} = \frac{\mathcal{R}}{1+\mathcal{R}^2} \qquad \text{and} \qquad \mathcal{B}' = \frac{\mathcal{R}^2}{1+\mathcal{R}^2}, \tag{5}$$

and is related to the usual drag parameter γ by the relation

$$\mathcal{R} = \frac{\gamma}{\kappa \rho_\mathrm{n}}. \tag{6}$$

Note that for $\mathcal{R} \ll 1$ (which is relevant in our context), one has $\mathcal{B} \approx \mathcal{R}$ and $\mathcal{B}' \ll \mathcal{B}$.

In our model, we shall consider the two components to be rotating around the same axis defined by $\hat{\Omega}_\mathrm{p}$. Furthermore, the protons in the crust (to which the magnetic field is assumed to be anchored) are bound in ions which form a crystalline solid and are connected to the protons in the core on an Alfvén crossing time-scale, which for a NS core is of the order of a few seconds (or possibly less if the core is superconducting) and thus much shorter than the dynamical time-scales we are interested in (except possibly for the glitch rise time). Accounting for the elastic forces in the crust and Alfvén waves in the core is clearly a prohibitive task, so as a first approximation we shall account for these effects by considering the proton conglomerate to be rigidly rotating. We make no such assumptions for the neutrons which will, in fact, develop differential rotation if vortices migrate to different regions of the star, as can be seen from equation (4).

Following Sidery et al. (2010), we can write the equations of motion for the angular frequency of the two components in the form

$$\dot{\Omega}_\mathrm{n}(\tilde{r}) = \frac{Q(\tilde{r})}{\rho_\mathrm{n}} \frac{1}{1-\varepsilon_\mathrm{n}-\varepsilon_\mathrm{p}}, \tag{7}$$

$$\dot{\Omega}_\mathrm{p}(\tilde{r}) = -\frac{Q(\tilde{r})}{\rho_\mathrm{p}} \frac{1}{1-\varepsilon_\mathrm{n}-\varepsilon_\mathrm{p}} - \frac{\mathcal{A}}{I_\mathrm{p}}\Omega_\mathrm{p}^3, \tag{8}$$

where we have defined

$$Q(\tilde{r}) = \rho_\mathrm{n} \kappa n_\mathrm{v} \mathcal{B}(\Omega_\mathrm{p} - \Omega_\mathrm{n}) \tag{9}$$

and

$$\mathcal{A} = \frac{B^2 \sin\theta^2 R^6}{6c^3}, \tag{10}$$

with B the surface magnetic field strength, θ the inclination angle between the field and the rotation axis and I_p the moment of inertia of the proton fluid in the star. Note that the coupling between the components depends only on the dissipative mutual friction coefficient $\mathcal{B}$ and not on $\mathcal{B}'$. If we now assume rigid rotation for the protons, i.e. a constant Ω_p, we can multiply equation (8) by $\tilde{r}^2 \rho_\mathrm{n}$ and integrate over the volume, thus recasting the system in the form

$$I_\mathrm{p}\dot{\Omega}_\mathrm{p} = -\frac{\mathcal{A}^3}{\Omega_\mathrm{p}} + \int \tilde{r}^2 Q(\tilde{r}) \frac{1}{1-\varepsilon_\mathrm{n}-\varepsilon_\mathrm{p}} \mathrm{d}V, \tag{11}$$

$$\dot{\Omega}_\mathrm{n}(\tilde{r}) = \frac{Q(\tilde{r})}{\rho_\mathrm{n}} \frac{1}{1-\varepsilon_\mathrm{n}-\varepsilon_\mathrm{p}}. \tag{12}$$

3 THE PINNING FORCE

Although vortex pinning in the crust has been suggested as the main mechanism behind pulsar glitches more than 20 years ago by Anderson & Itoh (1975), until recently very little work has been devoted to obtaining realistic estimates of the pinning force. The main difficulty lies in the fact that, although there have been several estimates of the pinning energy and thus of the force per pinning site (Alpar et al. 1984a), it is in fact the pinning force *per unit length* acting on a vortex that is the relevant quantity to compare with the Magnus force if one is to understand when a vortex line can unpin (Anderson et al. 1982).

In fact it has been argued by Jones (1997) that if one considers an infinitely long vortex line and averages over the various orientations with respect to the lattice, the pinning force will be negligible. Recent calculations by Grill & Pizzochero (in preparation) have shown that for realistic configurations in which one considers a vortex to be rigid over length-scales of 100–1000 Wigner–Seitz radii, the averaging process over mesoscopic length-scales and different orientations of the lattice does indeed reduce the strength of the pinning force with respect to previous estimates based on the pinning force per pinning site. However, the values obtained in these calculations, which are in fact the first realistic estimate of the pinning force per unit length, are still large enough to explain pulsar glitches (Pizzochero 2011).

It is beyond the scope of the present work to make a comparison between various superfluid gap models and equations of state [however, see the discussion in Pizzochero, Seveso & Haskell (in preparation); Seveso (2010), who find that the main qualitative features of the model remain unchanged], as at present we are mainly interested in understanding how to reproduce the main features of a glitch with a simplified large-scale hydrodynamical NS model. Furthermore, we shall use a Newtonian model to describe the mutual friction dissipation between the two components, as at present the relativistic prescription for doing this is not fully developed. Given the inaccuracies inherent to a Newtonian calculation of a NS model, any comparison between realistic equations of state would be at least dubious. Furthermore, there are, as we shall see, huge uncertainties associated with the values of the mutual friction coupling parameters that would make such a calculation meaningless.

In this work, we shall focus on the case of continuous straight vortices that thread the whole star, as in Pizzochero (2011), and extract the main features of the calculation of Pizzochero et al. (in preparation) to construct a simplified model for the maximum lag

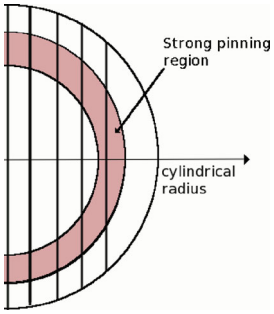

Figure 1. A schematic representation of the geometry of our problem. We show a NS section in which the shaded area represents the strong pinning region of the crust (out of scale). The star is threaded by straight continuous vortices. Clearly, the larger the portion of a vortex immersed in the pinning region, the stronger the effective pinning force, leading to a sharp maximum for large cylindrical radii, as shown in Fig. 2.

that can be developed. Note that we do not consider the possibility of a turbulent tangle of vortices, which would modify the vortex dynamics and the form of the mutual friction force (see e.g. Melatos & Peralta 2007). The inclusion of such effects is beyond the scope of this paper, but should clearly be the focus of future work.

In our picture, the maximum pinning force is obtained by balancing the Magnus force over a whole vortex, and the critical unpinning lag between the two components ($\Delta\Omega = \Omega_{\rm n} - \Omega_{\rm p}$) will have cylindrical symmetry and be a function of the cylindrical radius $\tilde{r} = r\sin(\theta)$ only. Close to the rotation axis, the radial behaviour is thus due to the Magnus force, as the vortices encounter a roughly similar number of pinning sites. The critical lag thus falls off as $\approx 1/\tilde{r}$ until it reaches a minimum value of $\Delta\Omega \approx 10^{-4}\,{\rm rad\,s^{-1}}$ at the base of the crust [note that in the analytic model of Pizzochero et al. (in preparation), the minimum is at somewhat higher densities, deeper in the outer core]. The critical lag then rises steeply in the equatorial region as the vortices are now completely contained in the pinning region (as illustrated schematically in Fig. 1) and reaches a maximum value of $\Delta\Omega \approx 10^{-2}\,{\rm rad\,s^{-1}}$, in the inner crust. We model this behaviour as a linear rise of the lag between the minimum and maximum values. As we continue to move outwards, the lag then decreases linearly again as the vortices annihilate in the outer regions of the crust where the neutrons are no longer superfluid. A schematic representation of this is given in Fig. 2.

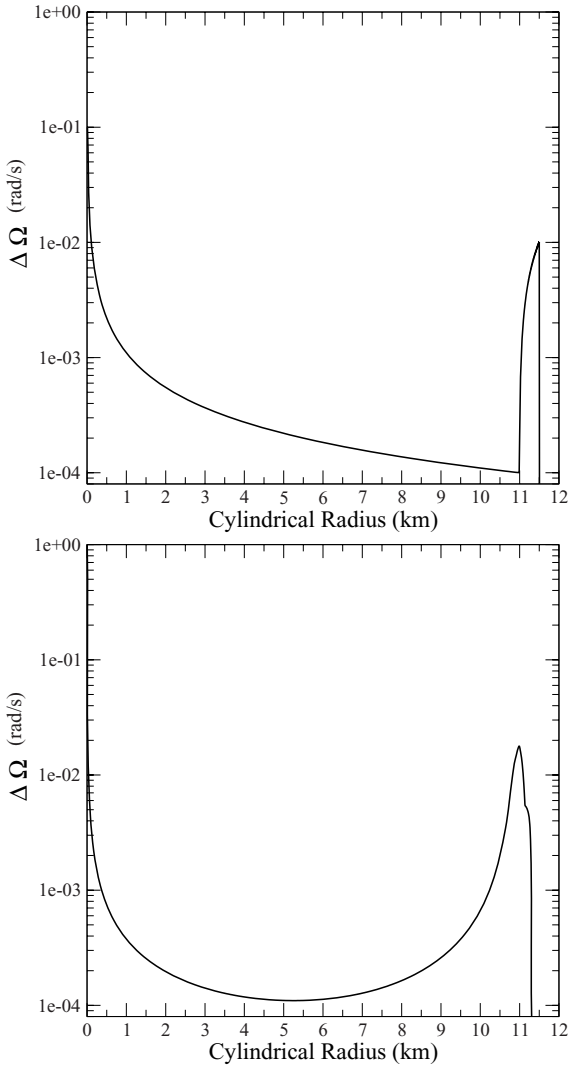

Figure 2. The top panel shows our approximation of the critical unpinning lag $\Delta\Omega = \Omega_{\rm n} - \Omega_{\rm p}$ for a 12 km, 1.4 $\rm M_\odot$ star, modelled as an $n = 1$ Newtonian polytrope. In the bottom panel, we show for comparison the critical unpinning lag for a realistic model of a 12 km, 1.4 $\rm M_\odot$ star obtained by solving the Tolman–Oppenheimer–Volkoff equations and using the SLy equation of state (Chabanat et al. 1998) as discussed in Pizzochero et al. (in preparation).

4 EQUATION OF STATE AND DRAG PARAMETERS

Let us discuss the fiducial NS model that we adopt for our calculations. We consider a 1.4 $\rm M_\odot$, with a radius $R = 12\,{\rm km}$, and assume that the base of the pinning region is at $r = 11.15\,{\rm km}$, at a density $\rho = 9.6 \times 10^{13}$, which is roughly consistent with the estimates of Pizzochero et al. (in preparation). We take the background equation of state of our NS to be an $n = 1$ polytrope, which allows us to make use of the explicit solution for the density profile:

$$\rho = \rho_{\rm c}\frac{\sin\alpha}{\alpha}, \tag{13}$$

with

$$\alpha = \frac{\pi r}{R} \quad \text{and} \quad \rho_{\rm c} = \frac{\pi M}{4R^3}. \tag{14}$$

This gives us a value $I_{\rm t} = 1.57 \times 10^{45}$ for the total moment of inertia. However, we need to consider the proton and neutron densities separately, so, following Reisenegger & Goldreich (1992), we shall consider a proton fraction $x_{\rm p}$ of the form

$$x_{\rm p} = \frac{\rho_{\rm p}}{\rho} = 0.05\left(\frac{\rho}{10^{14}\,{\rm g\,cm^{-3}}}\right), \tag{15}$$

where $\rho = \rho_{\rm p} + \rho_{\rm n}$ is the total density.

Finally, in a fully consistent model, one should be able to obtain the entrainment coefficients directly from the equation of state. There are, however, few realistic fully consistent equations of state for superfluid NS matter. Entrainment coefficients have, however, been obtained for the cores of stars containing hyperons (Gusakov, Kantor & Haensel 2009a,b), and for the crust one can rely on calculations of the proton effective mass (Chamel 2006; Chamel & Carter 2006; Chamel, Pearson & Goriely 2011) which is related to our entrainment coefficients by the relation (Prix, Comer & Andersson 2002)

$$\varepsilon_{\rm p} = 1 - \frac{m_{\rm p}^*}{m_{\rm p}}, \tag{16}$$

where m_p is the bare proton mass and m_p^* is the proton effective mass. Recent calculations by Chamel (2006) suggest that the proton effective mass is slightly lower than the bare mass in the core but can be larger in the crust. This means that the entrainment parameters will vanish close to the base of the crust (Carter, Chamel & Haensel 2006). As this is the region we are mainly interested in for our evolutions and given the introductory nature of this work, we shall take $\varepsilon_p = \varepsilon_n = 0$.

The discussion of the mutual friction coefficients is more complex. The mechanisms that give rise to mutual friction are in fact different in different regions of the star. In the core, we expect electron scattering of vortices to be at work, coupling neutrons and protons on a time-scale of $\tau \approx 10$ rotational periods (Alpar et al. 1984b; Andersson et al. 2006) (which for the Vela pulsar would give a time-scale of slightly less than a second). Another possibility is that, if the protons are in a type II superconducting state, the interaction between flux tubes and vortices will couple the two components on an even shorter time-scale (Sidery & Alpar 2009), although if the flux tube tangle is sufficiently strong to 'pin' the vortices this may lead to the opposite being true and the core being effectively decoupled for most of the evolution (Ruderman et al. 1998; Link 2003). We shall discuss this possibility in more detail in the following.

In the crust, on the other hand, it has been shown by Jones (1992) (see also Jones 1990; Epstein & Baym 1992) that coupling to sound waves in the lattice will be the main source of dissipation for low velocities of the vortices with respect to the lattice ($\leq 10^2$ cm s^{-1}), while dissipation due to the excitation of Kelvin waves in the vortices will dominate for large relative velocities.

In Table 1, we show the values of the drag parameters in the crust, for both these interactions, obtained from Jones (1990) by using recent values of the vortex–nucleus interaction (Donati & Pizzochero 2006). Unfortunately, there is a large uncertainty associated with this calculation, as one must not only evaluate the energy dissipated by the interaction of the vortex with a single pinning site, but also sum coherently over the length-scale associated with vortex rigidity [which Grill & Pizzochero (in preparation) and Grill (2011) find to be of the order of 10^2–10^3 Wigner–Seitz radii]. The summation procedure leads to a poorly constrained reduction factor δ, which Jones (1990) finds to be of the order of $\delta \approx 10^{-4}$. This is consistent with the results of Grill & Pizzochero (in preparation), who find that averaging over mesoscopic vortex length-scales and different crystal orientations leads to a reduction of up to two orders of magnitude in the pinning force per unit length compared to previous estimates that were obtained directly from the pinning force per pinning site. Given the scalings in the expressions for the drag parameters of Jones (1990), this would lead to a reduction factor $\delta \approx 10^{-4}$ for the drag parameters. There is thus a large uncertainty associated with the values in Table 1 and, furthermore, drag parameters $\mathcal{R} \gg 1$ are dubious as for such a strong interaction the perturbative treatment of Jones (1990) breaks down (Epstein & Baym 1992). This suggests that for our qualitative study, we may take a constant drag parameter throughout the crust and study how the results depend on its variation.

Table 1. Drag parameters in the crustal regions defined by Negele & Vautherin (1973). In the last two lines, we have applied a reduction factor $\delta = 10^{-4}$, as described in the text. $\mathcal{R}_p$ indicates the drag parameter due to phonon excitations and $\mathcal{R}_k$ that due to Kelvin excitations.

Zone	1	2	3	4	5
ρ ($\times 10^{14}$ g cm^{-3})	0.015	0.096	0.34	0.78	1.3
$\mathcal{R}_p$ ($\times 10^{-5}$)	1.6	0.7	5.8	0.025	0.0
$\mathcal{R}_k$ ($\times 10^2$)	290	5.8	340	0.085	0.0
$\mathcal{B}_p$ ($\times 10^{-5}$)	1.6	0.7	5.8	0.025	0.0
$\mathcal{B}_k$ ($\times 10^{-2}$)	0.003	0.18	0.003	11.64	0.0
$\delta = 10^{-4}$					
$\mathcal{B}_p$ ($\times 10^{-9}$)	1.6	0.7	5.8	0.025	0.0
$\mathcal{B}_k$ ($\times 10^{-2}$)	30.8	5.8	27.1	0.04	0.0

In particular, we shall consider values in the region $\mathcal{B}_p \approx 10^{-10}$ for the weak drag due to the interaction with lattice phonons and $\mathcal{B}_k \approx 10^{-3}$ for the strong drag due to Kelvin wave excitation. For the core, on the other hand, we shall consider electron scattering off vortex cores as the main source of dissipation (Alpar, Langer & Sauls 1984b). In this case, we take for the mutual friction coefficient (Andersson et al. 2006)

$$\mathcal{B}_c = 4 \times 10^{-4} \left(\frac{\delta m_p^*}{m_p}\right)^2 \left(\frac{\delta m_p^*}{m_p^*}\right)^{1/2} \left(\frac{x_p}{0.05}\right)^{7/6} \rho_{14}^{1/6}, \quad (17)$$

where m_p^* is the effective proton mass, $\delta m_p^* = m_p^* - m_p$ and ρ_{14} is the density in units of 10^{14} g cm^{-3}. However, given that we are already taking the drag parameter to be a constant in the crust, we shall also consider constant drag in the core. This choice is more than adequate given that we are not using a realistic prescription for the density profile or the effective mass. We shall thus consider drag parameters in the region of $\mathcal{B}_c \approx \mathcal{R}_c \approx 5 \times 10^{-4}$. Note that microscopically the exact nature of the superconductor in the NS interior is still open to debate (Jones 2006). The values we use are consistent with the core being in a type I superconducting state (Sedrakian 2005) [although see Jones (2006), for a discussion of strong drag in a type I superconductor] and with the possibility that one has a type II superconductor and the drag is strong, either as a consequence of the magnetic field geometry (Sidery & Alpar 2009) or due to a significant number of vortices cutting though the magnetic flux tubes. We do not consider here the possibility that vortices are strongly pinned to flux tubes in a type II superconductor and the most of the core is thus decoupled from the crust. This is clearly an interesting possibility which shall be the object of future work.

In our model, the exact value of the drag parameter acting on a vortex section depends critically on the region we are considering, as not only do the parameters depend on density, but the very nature of the drag varies from crust to core. We shall therefore integrate over a whole vortex and define an 'effective' drag coefficient which depends only on cylindrical radius (as shown in Fig. 3) by averaging over the vortex length. Our effective drag parameter thus depends mainly on how sizeable a portion of the vortex is immersed in the core (i.e. the stronger drag region) rather than in the crust.

5 DESCRIPTION OF THE MODEL

5.1 Core

Let us now describe the evolution of the system as it spins down due to the electromagnetic torque. First of all, let us focus on the central regions of the star. Here the vortices will stretch through the fluid core and only a small portion will experience pinning to the crustal lattice. This set-up is in fact very similar to that used to study the spin-up of superfluid helium in a container. In this case, the vortices are only pinned to the surface of the container and unpin once the Magnus force integrated over a vortex is approximately equal in magnitude to the tension (see e.g. Adams, Cieplak & Glaberson

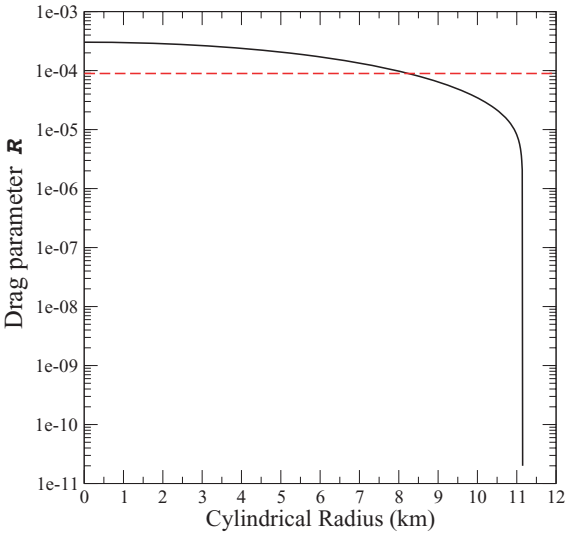

Figure 3. The average drag parameter $\mathcal{R}$ as a function of cylindrical radius, obtained by averaging the core contribution $\mathcal{R}_c$ and crust contribution $\mathcal{R}_p$ over the length of a vortex. Note that we consider only the drag due to phonon excitation ($\mathcal{R}_p$) in the crust as we are assuming that Kelvin waves can only be excited once the maximum critical unpinning lag has been exceeded. The horizontal line corresponds to $\mathcal{R}$ of the order of 10^{-4}, which gives a coupling time-scale of the order of 1 min for the Vela pulsar.

1984; Sonin 1987):

$$T_L \approx \frac{\rho_n \kappa^2}{4\pi} \ln\left(\frac{b}{\xi}\right), \tag{18}$$

with b the intervortex spacing and ξ the vortex core radius. This is in fact natural as we can expect that once the Magnus force exceeds the tension, the vortex will no longer behave rigidly, but we can expect reconnection and Kelvin waves to be excited, possibly developing turbulence and leading to a number of vortices to unpin and begin to 'creep' radially outwards (Schwarz 1984) [although bundles of vortices could be significantly more rigid (Ruderman & Sutherland 1973)]. For average parameters, the Magnus force in the core will exceed the line tension almost immediately once a lag begins to develop ($\Delta\Omega_c \approx 10^{-13}$), leading to the conclusion that (as in ^{4}He) unpinned vorticity dominates for most of the time, and repinning can only take place if the two components are essentially comoving (i.e. $\Delta\Omega < \Delta\Omega_c$). Note that the situation is radically different in the crust, where the vortex line is fully immersed in the lattice and is pinned in several points. In this case, we can expect it to move freely only once the maximum pinning force of Section 3 is exceeded.

Let us, however, stress that the assumption of free vortices is not crucial for our model. One can, in fact, easily account for the fact that possibly not all vortices will be free to move, but at any given time only a small fraction will be free, and subject to the drag force. Following Jahan-Miri (2005, 2006), we shall assume that the instantaneous number density of free vortices n_m is given,

$$n_m = \xi n_{v,} \tag{19}$$

where n_v is the total number density of vortices and ξ is the fraction of unpinned vortices at a given time. By now averaging over time, we can obtain an effective mutual friction parameter $\mathcal{B}_E = \xi\mathcal{B}$. Note that in principle, ξ could be obtained from the standard thermal 'creep' model (Alpar et al. 1984a; Link, Epstein & Baym 1992). In the following, we shall, however, not attempt to model this, as there are huge theoretical uncertainties on the unpinning probability and observational constraints are also very model-dependent. Nevertheless, by varying ξ and thus reducing the 'effective' drag parameter, we can account for vortex 'creep' in the linear regime, which has been used to interpret the relaxation phase of Vela glitches (Alpar et al. 1989).

The details of the steady state are, however, not crucial for our formulation, which is fortunate as not only vortex creep but also vortex repinning is still poorly understood, although efforts are being made to tackle this problem (Sedrakian 1995; Link 2009). Eventually the system will settle down to an equilibrium state in which both fluids are spinning down at the same rate and the lag can be estimated, from equations (7) and (8), to be

$$\Delta\Omega(\tilde{r}) \approx -\frac{\dot{\Omega}}{2\mathcal{B}(\tilde{r})\Omega}, \tag{20}$$

where $\mathcal{B}$ is the effective (averaged) mutual friction parameter, and we have neglected the effect of entrainment and differential rotation in equation (4). We will see in the following that this is actually a very good approximation to the equilibrium lag.

5.2 Strong pinning region

The repinning region, i.e. the equatorial region in which the pinning force rises steeply, deserves a separate discussion. As the vortices encounter what is, effectively, a barrier, we shall assume that they repin almost immediately. As we discuss below, this is effectively a situation in which the vortices 'creep' steadily outwards, i.e. move outwards with, on average, a low velocity. This suggests that Kelvin–phonon interactions will be strongly suppressed and that we can consider weak mutual friction coefficients, due to interactions with lattice phonons, in the region $\mathcal{B}_p \approx \mathcal{R}_p \approx 10^{-10}$, as described in the previous sections and as done in Fig. 3.

In fact, as the drag description is not valid close to repinning (Link 2009), one could argue that the form of the mutual friction in (3) is also not valid. Strictly speaking, this is true, but, as the full problem of the motion of a vortex in a strong pinning potential is at present intractable, we shall assume that the coupling given by mutual friction with the weak drag given by the interaction with phonons in the lattice is a good approximation.

The whole discussion could also be made rigorous by following the approach of Andersson, Haskell & Samuelsson (2011) and assuming that an extra 'pinning' force is acting on the vortices and defining an effective mutual friction parameter. However, given that we do not have a consistent description of an effective pinning force (but only the maximum pinning force), we shall simply assume that all vortices are pinned below the critical velocity, and then relax to their steady-state configuration once the critical unpinning lag is exceeded. This is equivalent to assuming that below the critical velocity, only a very small fraction of the vortices can 'creep', which is reasonable due to the sharp rise in the pinning force.

This leads to the neutrons relaxing to their steady-state rotational rate on a time-scale $\tau_r \approx 1/2\Omega\mathcal{B} \approx 10^8$ s (for $\mathcal{B} \approx 10^{-10}$ and assuming the rotation rate of the Vela pulsar, i.e. $\nu \approx 11$ Hz). During this time, the protons will have spun down, increasing the difference in rotational rate between the proton fluid and the neutrons that are still pinned. Given the strong radial dependence of the critical unpinning lag, this leads to vortices in regions further out in the star unpinning, while the inner regions are still relaxing to their equilibrium state. Essentially, one has an unpinning 'front' that is moving out radially. To obtain a simple estimate, let us assume that the front moves at approximately a constant speed $v_r = \Delta r/\tau_g$, with $\tau_g = \Delta\Omega_{max}/|\dot{\Omega}|$, which leads to a speed of approximately

$v_r \approx \dot{\Omega}\Delta r/\Delta\Omega_{\rm max} \approx 10^{-4}\,{\rm cm\,s^{-1}}$, where $\Delta r = 400\,{\rm m}$ is the width of the strong pinning region and $\Delta\Omega_{\rm max} \approx 10^{-2}$ is the maximum in the lag in the equatorial region (i.e. the front sweeps the whole pinning region in the time it takes for the lag to reach the maximum critical value). Note that we have also used the spin-down rate appropriate for the Vela pulsar, i.e. $\dot{\nu} \approx 10^{-11}\,{\rm Hz\,s^{-1}}$.

This means that the vortices that have unpinned from parts of the star closer to the rotation axis are clustered in this region, over a length-scale $l \approx \tau_r v_r \approx 10^4\,{\rm cm}$. We shall assume that it is this region that gives rise to the glitch once the maximum lag is exceeded and the vortices can no longer be pinned, thus no longer 'creep', but are free to escape radially outwards. Naturally this is an approximate estimate and in a realistic set-up the speed of the unpinning 'front' will not be constant and depend on the radial profile of the pinning force and of the drag coefficients. However, given the simplified set-up we are using for this study, we shall see that the above argument can still provide us with a reasonable order of magnitude estimate of the size of the region that gives rise to the glitch.

5.3 Glitch

Once the maximum lag has been reached, we shall assume that the pinning force can no longer contrast the Magnus force and that the vortices move out. They very rapidly reach a state of corotation with the neutrons, leading to velocities of $\approx 10^4\,{\rm cm\,s^{-1}}$ with respect to the lattice. In this regime, Kelvin–phonon dissipation will certainly dominate and recouple the neutrons and protons on a very short time-scale, giving rise to the rapid exchange of angular momentum that characterizes the glitch. Consistently with our prescription for the electron–phonon dissipation, we shall take the mutual friction coefficient for Kelvin–phonons to be $\mathcal{B}_{\rm k} \approx 10^{-3}$, and assume that it acts only in the region that has not relaxed to a steady state, i.e. the region in which the lag is greater than the equilibrium value:

$$\Delta\Omega > -\frac{\dot{\Omega}}{2\mathcal{B}_{\rm p}\Omega}. \tag{21}$$

We can estimate the relaxation time-scale in the crust as $\tau = 1/2\Omega\mathcal{B}_{\rm p}$ and assume that the pinning front moves through the strong pinning region over a period of 3 years (the approximate waiting time between glitches for the Vela pulsar, which shall be the main focus of our investigation), i.e. with a velocity $v \approx 4\times10^{-4}\,{\rm cm\,s^{-1}}$. The region which is still relaxing to its equilibrium state will then have a thickness of

$$\Delta \approx v\tau \approx \frac{3\times10^{-6}}{\mathcal{B}_{\rm p}}. \tag{22}$$

For a drag parameter $\mathcal{B}_{\rm p} \approx 10^{-10}$, one would then have approximately all of the strong pinning region involved in the glitch. A more quantitative analysis is shown in Fig. 4 where we show the edge of the non-relaxed region as a function of the drag parameter, obtained by measuring where the lag between neutrons and protons deviates from the analytic estimate in (21). We cannot extend the numerical analysis to very weak drag; nevertheless, we see that the region becomes larger for weaker drag and that extrapolating our results, we would have the whole crust involved in the glitch for $\mathcal{B}_{\rm p} \approx 2\times10^{-10}$. The extrapolation was obtained by fitting a function of the form, inspired by the estimate in (21), $f(x) = a - b/(\mathcal{R}_{\rm p}/10^{-10})$, where the best-fitting parameters were $a = 34.77 \pm 13.7\,{\rm m}$ and $b = 955.8 \pm 101.9\,{\rm m}$, which are in reasonable agreement (within factors of a few) with the analytical estimate. We shall thus assume that for $\mathcal{B}_{\rm p} < 2\times10^{-10}$, Kelvin oscillations of the vortices can be excited in the whole strong pinning region.

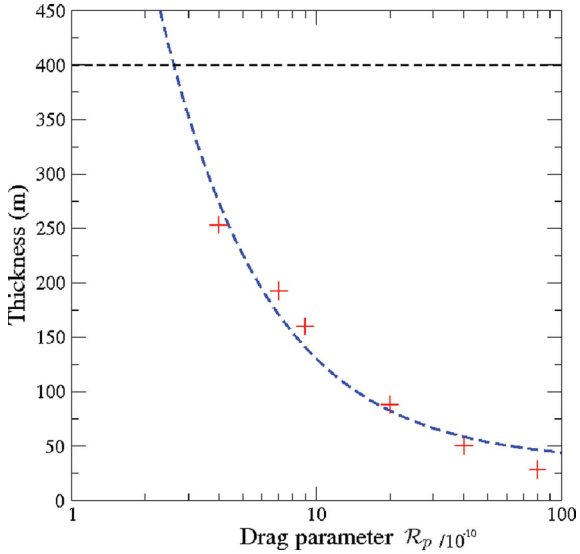

Figure 4. We plot the extent of the region in which Kelvin oscillations can be excited as a function of the weak drag parameter $\mathcal{R}_{\rm p}$. Note that the whole strong pinning region is 400 m thick, as indicated by the horizontal line. We extrapolate the value of the drag parameter for which the whole region is involved by fitting a function of the form, inspired by the estimate in (21), $f(x) = a + b/(\mathcal{R}_{\rm p}/10^{-10})$, where the best-fitting parameters were $a = 34.77 \pm 13.7\,{\rm m}$ and $b = 955.8 \pm 101.9\,{\rm m}$. As we can see, the whole strong pinning region participates in the glitch for $\mathcal{R}_{\rm p} < 2\times10^{-10}$, as expected from the analytical estimates.

5.4 Post-glitch relaxation

Subsequent to the glitch, neutrons and protons will still be in approximate corotation only in the interior regions that are coupled on time-scales shorter than the glitch rise time. In the exterior core, the lag between neutrons and protons will have decreased by a factor of $\Delta\Omega \approx 10^{-4}$ due to the glitch itself (in fact, the proton fluid may now be rotating faster than the neutron fluid in some parts of the star). The neutrons and protons then return to their steady-state configurations with the time-scale appropriate to the average mutual friction parameter $\mathcal{B}$ of Fig. 3, at the cylindrical radius we are considering, thus naturally recoupling the core on time-scales that range from the glitch rise time in the innermost regions to months in the outermost regions (i.e. $\tilde{r} \approx 11\,{\rm km}$). As far as the strong pinning region is concerned, we shall assume that the vortices repin after the glitch, and gradually unpin (or begin to 'creep') again as a lag builds up due to the protons' spinning down. As already discussed, the details of the repinning are highly uncertain, but given the weak coupling in the crust, the details of such a mechanism will only impact on the longer relaxation time-scales.

6 RESULTS

In order to set up the pre-glitch conditions for our system, we impose that the two fluids rotate at the same rate and then begin to evolve in time. This would clearly not be the correct condition if, say, we are considering the situation immediately following a previous glitch. However, as we are setting up the situation for the next glitch, we are only interested in obtaining a steady state on long time-scales (i.e. the interglitch time-scale, which is approximately 3 years for the Vela pulsar). As we intend to evolve the system for approximately 3 years, we cannot evolve the whole interior, which would require us to deal with coupling time-scales of seconds, but assume that it is always coupled to the crust by including its moment of inertia in

that of the charged component, and only evolve the region between $\tilde{r} = 11.15$ and 11.55 km (i.e. the outer core in which the value of the drag parameter becomes small and varies rapidly, and the strong pinning region of the inner crust, up to the maximum of the critical lag). We neglect the outer crust, which we do not expect to be a bad approximation, as its moment of inertia is small compared to that of the other regions of the star. The equations of motion are thus integrated only up to the maximum of the pinning force, where we impose that the spatial derivative of the neutron angular velocity must vanish, i.e. $\partial\Omega_{\rm n}/\partial r = 0$, which is appropriate if the vortices are still pinned at that point. Note that this condition requires the vortices to be pinned homogeneously and thus assumes an abundance of available pinning sites. At every time-step, we thus evaluate the integral in (11) and then evolve the coupled equations in (11)–(12) forward in time with a four-step Runge–Kutta algorithm.

Once the maximum of the lag in the strong pinning region is reached, we initiate the glitch by switching to strong Kelvin drag ($\mathcal{B}_{\rm k}$) in the region that has not relaxed, i.e. the region for which $\Delta\Omega > -\dot{\Omega}/2\mathcal{B}_{\rm p}\Omega$. At this point, we track the evolution of the whole core by extending the numerical grid and filling the region that has not previously been evolved with the prescription $\Delta\Omega = -\dot{\Omega}/2\mathcal{B}_{\rm c}\Omega$. As can be seen in Fig. 5, this is indeed a good approximation for the initial condition, given that the time-scale on which the interior reaches a steady state is considerably shorter than the interglitch time-scale. When the strong drag regions have reached their equilibrium lag, we switch off the Kelvin drag and assume that the vortices have repinned. We then follow the immediate post-glitch relaxation by evolving the whole star over a time-scale of days.

Schematically, the procedure is as follows.

(i) Initially corotating fluids are evolved in time with a constant external spin-down torque acting on the charged component. In the crust, we check at each time-step if a grid point is above or below the critical unpinning lag at that radius, i.e. if $\Delta\Omega(\tilde{r}) > \Delta\Omega_{\rm crit}(\tilde{r})$.

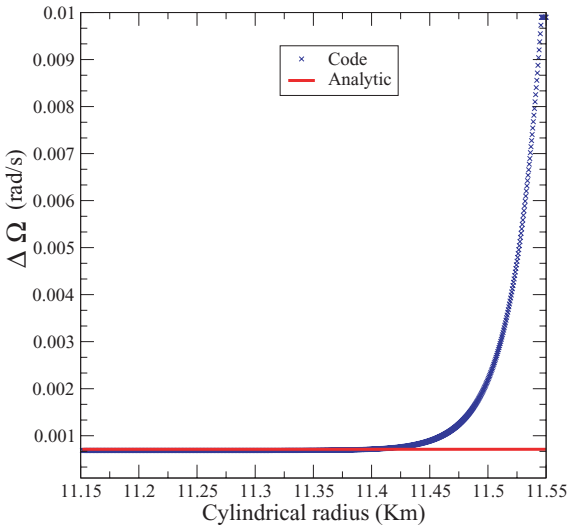

Figure 5. We compare, in the strong pinning region of the crust, the analytical prediction for the lag $\Delta\Omega$ between neutrons and protons to the value obtained in our simulations just before the glitch. The calculation was performed for $\mathcal{B}_{\rm p} = 10^{-9}$. As can be seen from the figure, the analytical estimate is a very good approximation, except for the outer region in which the system has not yet reached equilibrium. It will thus be a good approximation for the core, in which the coupling time-scale between neutrons and protons is considerably shorter than in the crust.

If it is below, the region is pinned and the neutrons are evolved with the rule $\dot{\Omega}_{\rm n} = 0$. If the lag has exceeded the critical lag, the full system of coupled equations is evolved, with $\mathcal{B} = \mathcal{B}_{\rm p}$.

(ii) Once the maximum unpinning lag has been reached, we initiate the glitch. We identify the region of the crust that has not yet relaxed to its steady state, as set by the weak phonon drag, i.e. the region in which $\Delta\Omega > -\dot{\Omega}/2\mathcal{B}_{\rm p}\Omega$. In this region, we set $\mathcal{B} = \mathcal{B}_{\rm k}$. We thus allow for strong Kelvin drag and rapid recoupling.

(iii) In the crustal regions for which we have set $\mathcal{B} = \mathcal{B}_{\rm k}$, we check at each time-step which grid points have reached equilibrium, as set by the strong drag coefficient this time. If this is the case, i.e. if $\Delta\Omega \approx -\dot{\Omega}/2\mathcal{B}_{\rm k}\Omega$, we assume that the region has repinned and $\dot{\Omega}_{\rm n} = 0$.

(iv) The procedure continues and in the pinned regions, we check if the lag has exceeded the critical unpinning lag, in which case we evolve the full coupled equations with $\mathcal{B} = \mathcal{B}_{\rm p}$ (i.e. with weak phonon coupling).

To summarize, we set up a system of corotating fluids with pinned vortices in the crust and evolve it in time. As the lag increases, the depinning front moves through the crust. Once the maximum critical lag is reached, the vortices move rapidly outwards and strong Kelvin mutual friction recouples the components, giving rise to the glitch. After the glitch, the lag has decreased throughout the star and each region relaxes to equilibrium on a time-scale determined by the local values of the (average) mutual friction.

6.1 The Vela pulsar

Let us first of all examine the case of the Vela pulsar, which is the prototype system for giant glitches. The Vela (PSR B0833−45 or PSR J0835−4510) has a spin frequency $\nu \approx 11.19$ Hz and spin-down rate $\dot{\nu} \approx -1.55 \times 10^{-11}$ Hz s^{-1}. Giant glitches are observed roughly every 2–3 years and have relative frequency jumps of the order of $\Delta\nu/\nu \approx 10^{-6}$. The spin-up is instantaneous to the accuracy of the data, with the best constraint being an upper limit of 40 s for the rise time obtained from the 2000 glitch (Dodson et al. 2001) [a similar upper limit of 30 s was obtained from the analysis of the 2004 glitch, but was less significant due to the quality of the data (Dodson et al. 2007)]. The glitch is usually fitted to a model consisting of permanent steps in the frequency and frequency derivative and a series of transient terms that decay exponentially. It is well known that at least three are required to fit the data, with decay time-scales that range from months to hours (Flanagan 1996). Recent observations of the 2000 and 2004 glitch have shown that an additional term is required on short time-scales, with a decay time of approximately a minute. The fitted values for the relaxation of these two glitches are shown in Table 2. The spin-down rate always increases after a glitch with larger relative increases (up to a factor of 10) which decay on the shorter time-scales and smaller (a few per cent) increases that decay on the longer time-scales of days and months. Note that a further two glitches were detected in 2008 and 2010, but no timing analysis has yet been published.

Consistently with the results of Grill & Pizzochero (in preparation), Grill (2011) and Pizzochero (2011), we take the maximum of the critical unpinning lag to be $\Delta\Omega_{\rm c} = 10^{-2}$, which naturally leads to a glitch recurrence time of roughly 3 years (the exact time depends on the choice of drag parameters, but is always approximately 1100 d). Our simulations can then reproduce glitches with fractional rises $\Delta\nu/\nu \approx 10^{-6}$ for a range of parameters. In Fig. 6, we show the rise time and the 'instantaneous' size of the glitch, i.e. the size at the end of the rise, as a function of the strong Kelvin

Table 2. The fitted values for the relaxation of the Vela 2000 and Vela 2004 glitches from Dodson et al. (2001) and Dodson et al. (2007). After removing the pre-glitch spin-down, the fit on the residuals is performed with a function of the type $f(t) = \Delta_p F + \Delta_p \dot{F} t + \sum_i f_i \exp(-t/\tau_i)$.

	2000	2004
$\Delta_p F$ (Hz)	3.454 35E−05	2.2865E−05
$\Delta_p \dot{F}$ (Hz s^{-1})	−1.0482E−13	−1.0326E−13
f_1 ($\times 10^{-6}$ Hz)	0.02	54
f_2 ($\times 10^{-6}$ Hz)	0.31	0.21
f_3 ($\times 10^{-6}$ Hz)	0.193	0.13
f_4 ($\times 10^{-6}$ Hz)	0.2362	0.16
τ_1	1.2 ± 0.2 min	1 ± 0.2 min
τ_2	0.53 d	0.23 d
τ_3	3.29 d	2.10 d
τ_4	19.07 d	26.14 d

drag parameter $\mathcal{R}_k$. As expected, the larger the drag parameter, the shorter the rise time and the larger the glitch. This is simply due to the fact that the faster the glitch (or rather the stronger the Kelvin drag parameter with respect to the drag in the core), the smaller the fraction of the core superfluid neutrons that can remain coupled to the crust and contribute to its moment of inertia during the glitch.

However, a strong Kelvin drag will lead to rise times of the order of seconds, well below the observational upper limit of 40 s and thus well below the observational capabilities of current radio telescopes that can, for the Vela pulsar, at best deal with 10-s folds. The rise will then be followed by a rapid relaxation. In fact, if we then extract the glitch size 40 s after the glitch is initiated, as shown in Fig. 7, we see that the situation is reversed. The stronger the drag, the smaller the glitch after 40 s, as an initially larger jump in frequency relaxes faster and leads, in fact, to a lower frequency after 40 s, which is illustrated in Fig. 8. In Fig. 7, we also see that stronger phonon drag parameters in the crust gives rise to smaller glitches, as more of the crust has relaxed to its equilibrium configuration and less angular momentum is available to be exchanged.

While the magnitude of the strong Kelvin drag affects mainly the glitch size and rise time, the strength of the drag in the core will affect, as shown in Figs 9 and 10, the size of the glitch itself (as it determines the amount of core superfluid that participates in the glitch) but also crucially affect the short-term post-glitch relaxation. In Fig. 10, we can see that a weaker drag in the core leads to less of the superfluid coupling to the crust and thus to a larger glitch, which however relaxes, on a time-scale of several minutes, more than in the case of stronger coupling. Unfortunately, the short time-scale component of the relaxation is not strongly constrained by observations, as it was only measurable in the 2000 and 2004 glitches, with vastly different magnitudes, as can be seen from Figs 11 and 12. The results in Fig. 12 would, however, indicate that a core drag parameter $\mathcal{R}_c \approx 10^{-5}$ is still marginally consistent with observation, but that there is no evidence for a much weaker drag, due for example to the fact that most vortices are pinned (either to the crust or to flux tubes in the core) and only a small fraction of them can creep. It would thus appear that the observations of the short-term relaxation are consistent with a mutual friction drag in the range $\mathcal{R}_c \approx 10^{-4} - 10^{-3}$, consistent with theoretical expectations for electron scattering off vortex cores. This is encouraging, given the approximate treatment of the drag parameter in this work. Note, however, that quantitative statements are not easy to make as there is a large degeneracy between the various parameters that enter the model. For example, in Fig. 13 we show that the uncertainty on the time of the glitch, which is of about 30 s, can lead to an uncertainty on the value of the drag parameters.

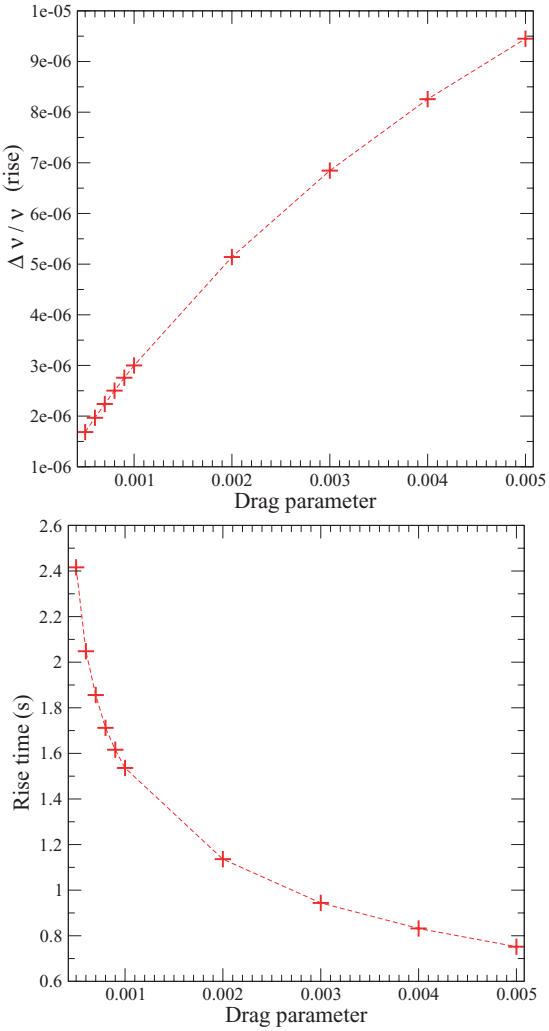

Figure 6. In the top panel, we plot the size of the glitch (at the end of the rise) and in the bottom panel the rise time, both as a function of the strong Kelvin drag parameter $\mathcal{R}_k$. For these simulations, we have taken $\mathcal{R}_p = 10^{-10}$ and $\mathcal{R}_c = 5 \times 10^{-4}$. Note that the segments joining the points are to guide the eye only, and not the result of a fitting procedure.

In Fig. 11, we show the longer time-scale components of the relaxation. These also appear consistent with a strong core drag due to electron scattering, although a slower spin-down may be preferred on a time-scale of days. Quantitative statements regarding the longer relaxation time-scales (days to months) are, however, hindered by computational and theoretical issues. On the one hand, evolving the full system of coupled equations for longer than a few days is computationally challenging, on the other, theoretical uncertainties regarding repinning after a glitch and creep begin to have a significant impact on the results for these longer time-scales, while they do not affect short time-scales of minutes or hours. In order to obtain truly quantitative results for longer time-scales, it would be necessary to address these theoretical issues and also to include a realistic density dependence of the drag parameters. Finally, other effects are likely to play a role in the relaxation time-scale, notably friction at the crust–core interface (van Eysden & Melatos 2010), the inclusion of which would require us to relax

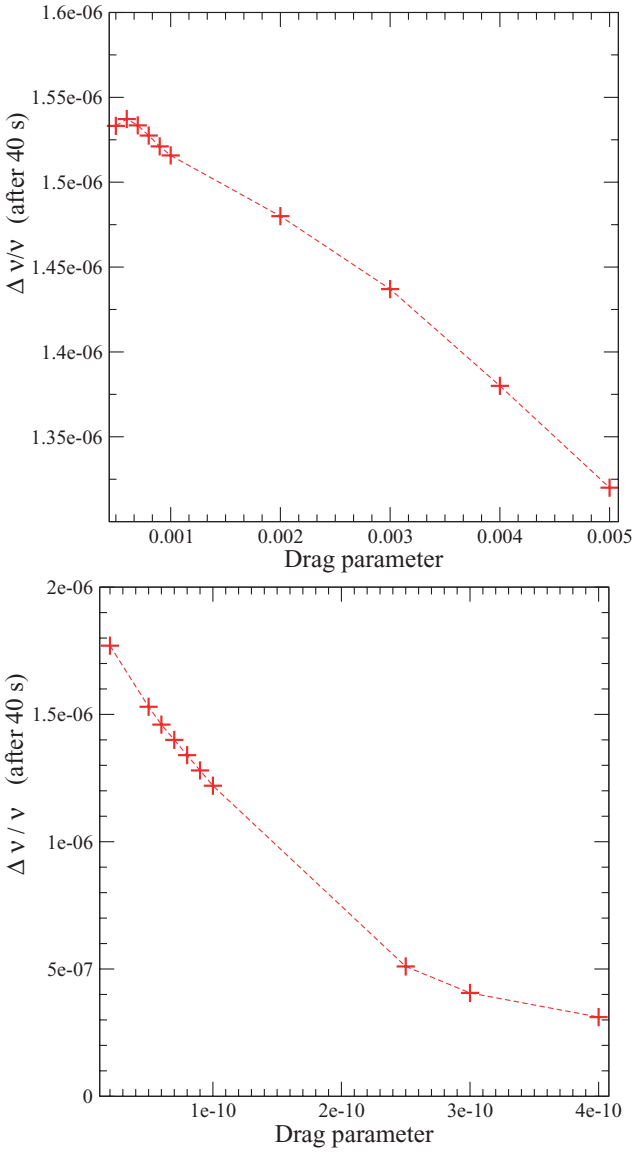

Figure 7. The size of the glitch, extracted 40 s after it is initiated, as a function of the drag parameters. In the top panel, we plot the glitch size as a function of the strong drag parameter $\mathcal{R}_k$. In this case, the stronger the drag, the smaller the glitch, as an initially larger glitch relaxes faster and is, in fact, smaller after 40 s. The remaining drag parameters were taken to be $\mathcal{R}_p = 5 \times 10^{-11}$ and $\mathcal{R}_c = 4 \times 10^{-4}$. In the bottom panel, we show the glitch size as a function of the weak drag parameter $\mathcal{R}_p$. Again for larger values of the drag, we obtain a smaller glitch, as in this case more of the fluid in the crust has relaxed to its equilibrium configuration prior to the glitch and less angular momentum is available to be exchanged. The remaining drag parameters were taken to be $\mathcal{R}_k = 6 \times 10^{-4}$ and $\mathcal{R}_c = 4 \times 10^{-4}$. Note that the segments joining the points are to guide the eye only, and not the result of a fitting procedure.

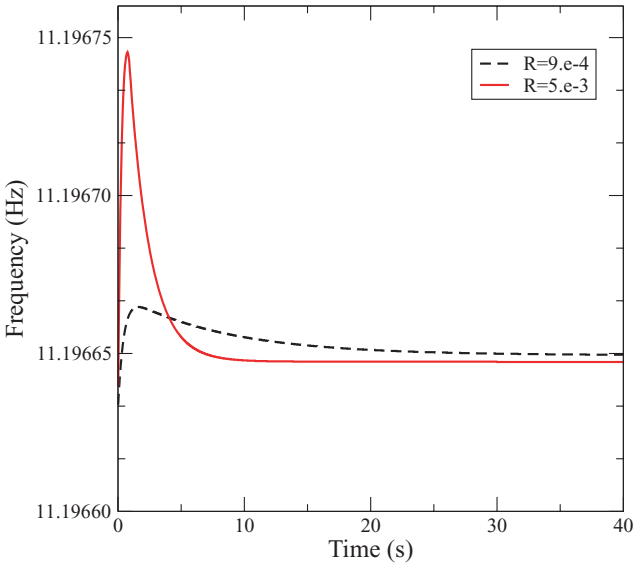

Figure 8. The first 40 s of the glitch for two values of the Kelvin drag parameter $\mathcal{R}_k$. A stronger drag (i.e. a shorter coupling time-scale) gives rise to an initially larger glitch that, however, rapidly relaxes to a lower spin rate than that of a glitch involving a weaker drag parameter.

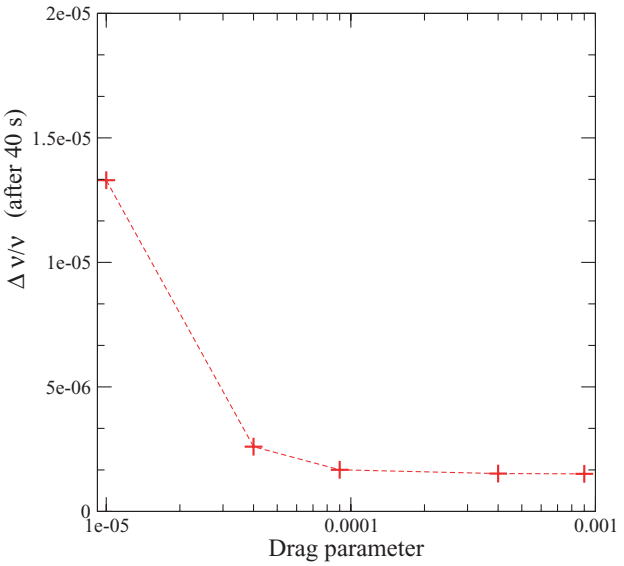

Figure 9. The size of the glitch, extracted 40 s after it is initiated, as a function of the core drag parameter. Weaker drag parameters give rise to larger glitches as less of the core can contribute to the moment of inertia during a glitch. The remaining drag parameters were set at $\mathcal{R}_p = 5 \times 10^{-11}$ and $\mathcal{R}_k = 1 \times 10^{-3}$. Note that the segments joining the points are to guide the eye only, and not the result of a fitting procedure.

the rigid rotation assumption for the charged component, which is beyond the scope of this paper but will be the focus of future work.

7 GIANT GLITCHERS

So far, we have only applied our model to the giant glitches of the Vela pulsar. Giant glitches have, however, been observed in several other pulsars and we would expect them to also occur when the system reaches the maximum critical lag for unpinning. As already mentioned, this need not be the case for smaller glitches that are likely to be due to random unpinning and may be, for example, described in terms of vortex avalanche dynamics (Warszawski & Melatos 2011). In fact, recent observations support the view that there is a bimodal distribution in the glitch size, with two different populations, the 'giant' glitchers and pulsars that only exhibit smaller glitches (Espinoza et al. 2011). We shall thus focus on the population of 'Vela-like' pulsars that show giant glitches, as defined by Espinoza et al. (2011), which are shown on the P–$\dot{P}$ diagram in Fig. 14. In particular, seven of these objects have multiple giant

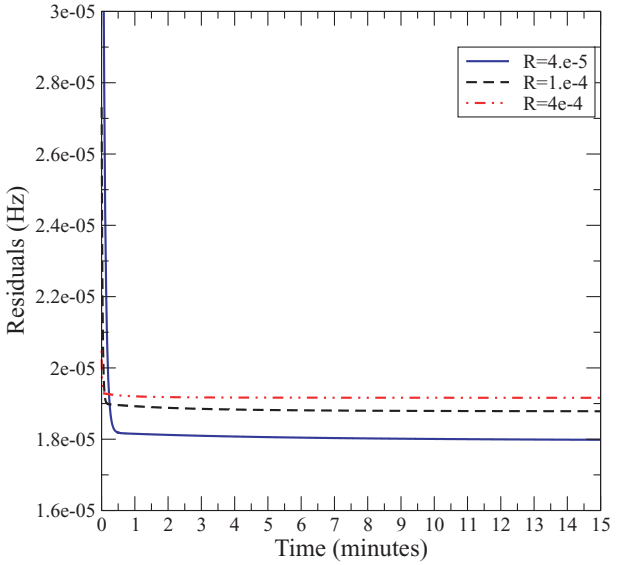

Figure 10. We plot the post-glitch residuals after subtracting the pre-glitch spin-down. The top panel shows the first 15 min of the relaxation for three values of the core drag parameter $\mathcal{R}_c$. We can see that a weaker drag in the core leads to less of the superfluid coupling to the crust and thus to a larger glitch, which however relaxes, on a time-scale of several minutes, more than in the case of stronger coupling.

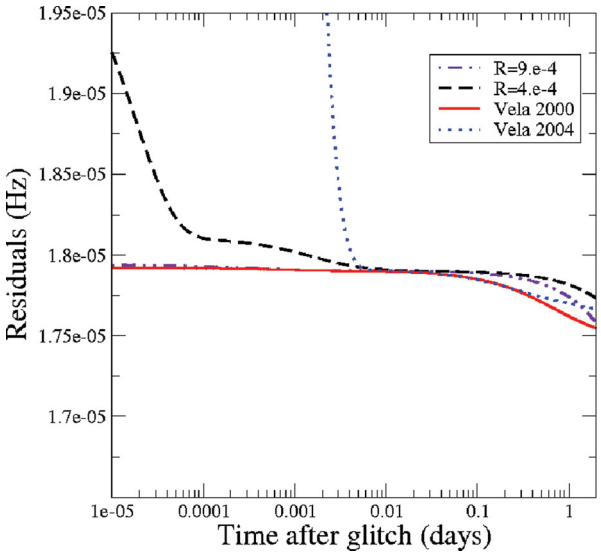

Figure 11. The post-glitch residuals, rescaled as in Fig. 12, but for a longer time-scale of 2 d.

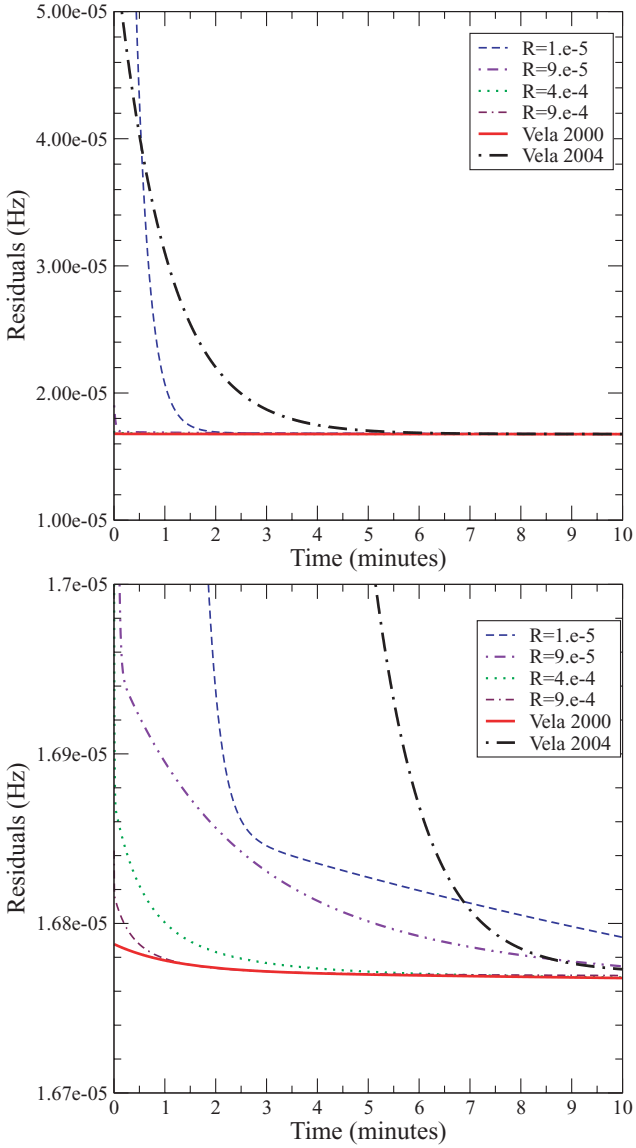

Figure 12. We plot the post-glitch residuals after subtracting the pre-glitch spin-down and having scaled all the results so that the glitch has decayed to the same frequency after 10 min. The bottom panel is a zoom-in of the top panel. It is clear that stronger drag parameters provide a better fit to the Vela 2000 relaxation fit (for which the data were of better quality) and that very weak drag parameters are still excluded by the Vela 2004 relaxation fit. It would appear that the observations are consistent with a drag parameter in the range $\mathcal{R}_c \approx 10^{-4}$ to 10^{-3}, as expected theoretically for electron scattering off vortex cores. A very weak drag, due to only a small fraction of the vortices' 'creeping', would not appear to be consistent with the short time-scale components of the relaxation.

glitches, and one can thus derive an approximate waiting time between glitches. In Fig. 15, we plot the waiting time as a function of the spin-down rate $\dot{\nu}$. The data appear consistent with our theoretical expectation that a pulsar that is spinning down faster will build up the critical lag on a shorter time-scale and glitch more often. In particular, we can see that most systems lie close to the Vela in the P–$\dot{P}$ diagram and also glitch roughly every few years, but the X-ray pulsar J0527–6910, which is spinning down approximately an order of magnitude faster glitches every few months, while the lower limits on slower pulsars indicate that they may glitch every decade.

Naturally, the situation will be complicated by the fact that these pulsars also exhibit smaller glitches, which may transfer part of the angular momentum before a giant glitch, and by the fact that the critical lag will also depend, albeit weakly (Pizzochero et al., in preparation), on the mass and radius of the star. Given these limitation, our model would, however, appear to be consistent with the observed inter(giant)glitch waiting time. Let us stress although data are available to study the distribution of waiting times for smaller glitches (see e.g. Melatos et al. 2008; Espinoza et al. 2011), we shall not present such a study here as our model only predicts the average waiting time of giant glitches, which are assumed to occur once the maximum critical lag is exceeded.

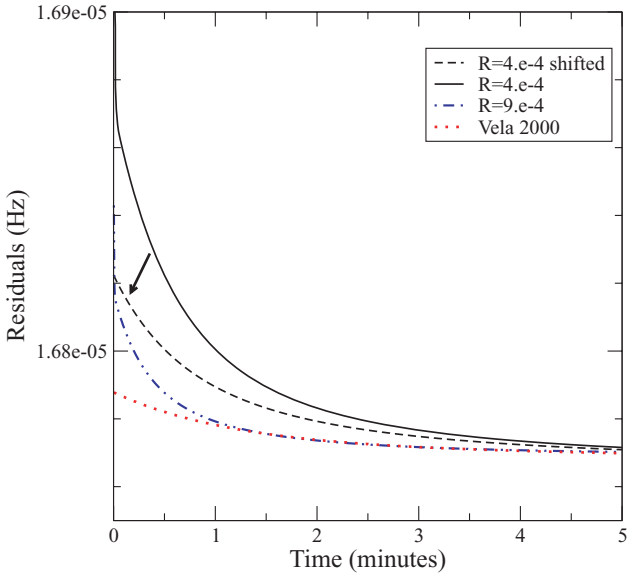

Figure 13. We plot the post-glitch residuals, rescaled as in Fig. 12, to illustrate the degeneracy between the assumed glitch epoch and the strength of the drag in the core. We show the effect of assuming that the glitch has occurred 30 s before the assumed epoch. We can see that the curve for $\mathcal{R}_c = 4 \times 10^{-4}$ now produces a smaller glitch and gives a better fit to the Vela 2000 data. The curve thus appears closer to that given by taking $\mathcal{R}_c = 9 \times 10^{-4}$ but not adjusting the glitch epoch.

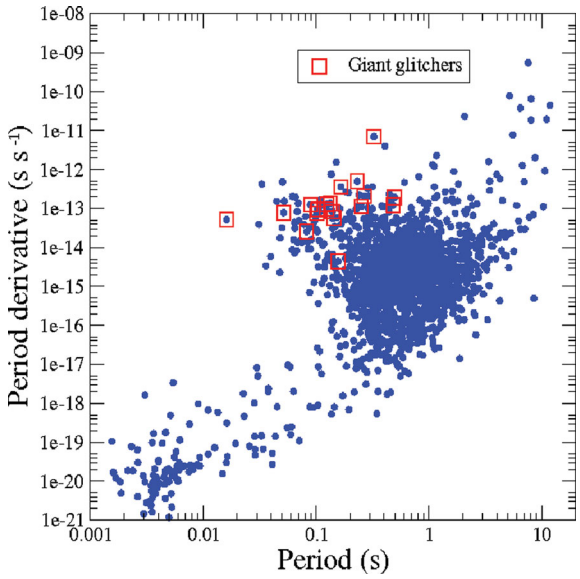

Figure 14. The location of the giant glitching pulsars as identified by Espinoza et al. (2011) in the P–$\dot{P}$ diagram. This is the population of pulsars that show large steps in the frequency ($\Delta\nu \approx 10^{-4}$ Hz) and always exhibit an increase in the spin-down rate after the glitch.

Unfortunately, only the Vela is currently observed at short enough intervals to allow a fit for the short time-scale transient terms in the relaxation, so more accurate tests are not currently possible for other pulsars. It would be of great interest if such observations for other giant glitchers were to become possible with the new generation of radio telescopes such as LOFAR and the SKA.

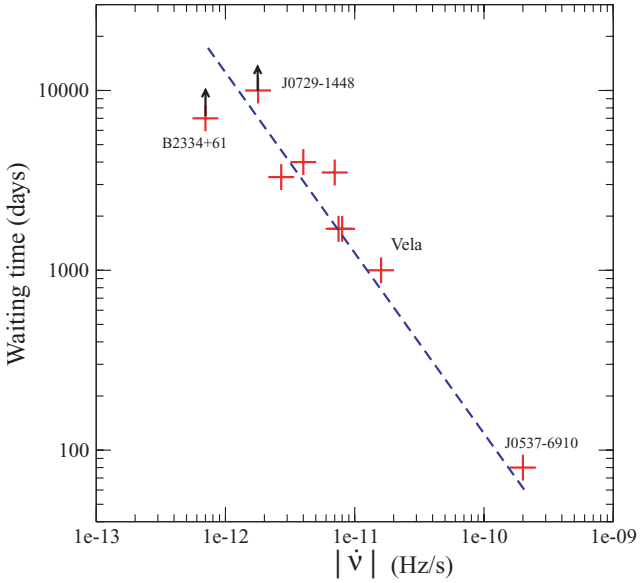

Figure 15. We plot the approximate waiting time between glitches for the pulsars that have shown multiple giant glitches, as a function of the spin-down rate. We also include two pulsars that have shown only one glitch but also have a long baseline for the observations and can thus provide us with an interesting lower limit on the waiting time. The data appear consistent with the notion that giant glitches can occur once a critical lag of approximately $\Delta\Omega = 10^{-2}$ is reached. In fact, the Vela-like pulsars glitch every few years, but the X-ray pulsar J0527−6910, which is spinning down approximately an order of magnitude faster, glitches every few months, while the lower limits on slower pulsars indicate that they may glitch every decade. In fact, the data appear to be well described by a fit of the form $y = A/x$, as shown in the figure, with y the waiting time in seconds, x the frequency derivative and $A = 1.082\,212 \times 10^{-3}$ Hz.

8 CONCLUSIONS

We have presented a hydrodynamical two-fluid model of pulsar glitches that can consistently model all phases of the glitch itself. Our model can be successfully applied to the giant glitches of the Vela pulsar, for which we can reproduce the approximate waiting time between glitches, the size of the glitch and the short-term post-glitch relaxation. The main assumption is that a giant glitch will occur once the system exceeds the maximum lag that the pinning force in the crust can sustain. This naturally gives rise to a waiting time between glitches that depends on the pulsar spin-down rate (i.e. it is the time it takes the crust to spin down by the required amount) and to a maximum size for the glitch. Both these quantities depend only weakly on the mass and radius of the star (Pizzochero et al., in preparation) and our model can, in fact, reproduce these features successfully also for the general population of 'giant glitchers', i.e. the pulsars for which giant glitches such as those of the Vela have been observed (Espinoza et al. 2011).

In our model, the coupling between the charged component (which we assume to be rigidly rotating) and the superfluid neutrons is given by the vortex-mediated mutual friction. Our results suggest that the mutual friction will be weak in the crust, possibly due to the fact that not all vortices are free, but rather that the strong pinning force gives rise to a situation in which most vortices are pinned and only a small fraction can 'creep' outwards. Only once the maximum unpinning lag is exceeded can the vortices move out freely, a process which can excite Kelvin oscillations and give rise to a strong drag and recoupling of the two components on a very short time-scale, i.e. a glitch. The short-term post-glitch relaxation

of the Vela, on the other hand, suggests that the magnitude of the drag in the core of the NS is consistent with theoretical expectations for electron scattering of magnetized vortex cores. Our model does not support the notion that, at least on short time-scales, a significant number of vortices is pinned in the core (as could, for example, be the case if one has a type II superconductor and vortices cannot cross flux tubes, effectively decoupling the core and the crust). A detailed analysis of the case in which the core consists of a type II superconductor will be a focus of future work in order to obtain more quantitative results and constraints on NS interior physics. Some vortices that cross the core may, however, be weakly pinned to the crust, and vortex repinning and creep (also in the core) may play a role on the longer time-scales associated with the recovery.

Another effect which will have an impact on the post-glitch recovery is the Ekman flow at the crust–core interface. This effect has been shown to be important in fitting the post-glitch recovery of the Vela and Crab pulsars by van Eysden & Melatos (2010), and future adaptations of our model should relax the rigid rotation assumption for the charged component and include the effect of Ekman pumping. Further developments should also include more realistic models for the drag parameters in the star, as the density dependence of the coupling strength clearly has an impact on the amount of angular momentum that can be exchanged on different time-scales. Truly quantitative results could then be obtained with the use of realistic equations of state together with consistent estimates of the pinning force, such as those of Grill & Pizzochero (in preparation) and Grill (2011).

Note that we have assumed that a giant glitch only occurs when the maximum critical lag is reached. If unpinning could be triggered earlier, this could generate smaller glitches. In fact, cellular automaton models have shown that the waiting time and size distributions of pulsar glitches can be successfully explained by vortex avalanche dynamics related to random unpinning events (Melatos & Warszawski 2009; Warszawski & Melatos 2010, 2011). In its present form, our model cannot predict such a distribution of glitch sizes and waiting times, but can describe successfully average glitch parameters and waiting times of giant glitches. It would thus be of great interest to use our long-term hydrodynamical models, with realistic pinning forces, as a background for such cellular automaton models that model the short-term vortex dynamics. Such a model could then also be extended to model not only large pulsar glitches, but more generally pulsar timing noise, an issue that is of great importance for the current efforts to detect GWs with pulsar timing arrays (Hobbs et al. 2010).

Finally, the next generation of radio telescopes, such as LOFAR and the SKA, is likely to provide much more precise timing data for radio pulsars and is likely to set much more stringent constraints on the glitch rise time and short-term relaxation, thus allowing us to test our models and probe the coupling between the interior superfluid and the crust of the NS with unprecedented precision.

ACKNOWLEDGMENTS

This work was supported by CompStar, a Research Networking Programme of the European Science Foundation.

BH would like to thank Cristobal Espinoza, Danai Antonopoulou and Fabrizio Grill for stimulating discussions on pulsar glitch observations and pinning force calculation. BH also acknowledges support from the European Union via a Marie-Curie IEF fellowship and from the European Science Foundation (ESF) for the activity entitled 'The New Physics of Compact Stars' (COMPSTAR) under exchange grant 2449.

TS acknowledges support from EU FP6 Transfer of Knowledge project 'Astrophysics of Neutron Stars' (ASTRONS, MTKD-CT-2006-042722).

REFERENCES

Adams P. W., Cieplak M., Glaberson W. I., 1984, Phys. Rev. B, 32, 171
Andersson N., Comer G. L., 2006, Classical Quantum Gravity, 23, 5505
Anderson P. W., Itoh N., 1975, Nat, 256, 25
Anderson P. W., Alpar M. A., Pines D., Shaham J., 1982, Philos. Magazine A, 45, 227
Andersson G., Sidery T., Comer G. L., 2006, MNRAS, 368, 162
Andersson N., Haskell B., Samuelsson L., 2011, MNRAS, 416, 118
Alpar M. A., 1977, ApJ, 213, 527
Alpar M. A., Anderson P. W., Pines D., Shaham J., 1981, ApJ, 249, L29
Alpar M. A., Anderson P. W., Pines D., Shaham J., 1984a, ApJ, 276, 325
Alpar M. A., Langer S. A., Sauls J. A., 1984b, ApJ, 282, 533
Alpar M. A., Cheng K. S., Pines D., 1989, ApJ, 346, 823
Avogadro P., Barranco F., Broglia R. A., Vigezzi E., 2007, Phys. Rev. C, 75, 012805
Baym G., Pines D., 1971, Ann. Phys., 66, 816
Baym G., Pethick C., Pines D., 1969, Nat, 224, 872
Bennett M. F., van Eysden C. A., Melatos A., 2010, MNRAS, 409, 1705
Carter B., Chamel N., Haensel P., 2006, Int. J. Modern Phys. D, 15, 777
Chabanat E., Bonche P., Haensel P., Mayer J. Schaeffer R., 1998, Nuclear Phys. A, 635, 231
Chamel N., 2006, Nuclear Phys. A, 773, 263
Chamel N., Carter B., 2006, MNRAS, 368, 796
Chamel N., Pearson J. M., Goriely S., 2011, in Alpar M. A., ed., AIP Conf. Ser. Vol. 1379, Astrophysics of Neutron Stars 2010. Am. Inst. Phys., New York, p. 27
Cheng K. S., Chau W. Y., Zhang J. L., Chau H. F., 1992, ApJ, 396, 135
Dodson R. G., McCulloch P. M., Lewis D. R., 2001, ApJ, 564, L85
Dodson R. G., Lewis D. R., McCulloch P. M., 2007, Ap&SS, 308, 585
Donati P., Pizzochero P. M., 2003, Phys. Rev. Lett., 90, 211101
Donati P., Pizzochero P. M., 2004, Nuclear Phys. A, 742, 363
Donati P., Pizzochero P. M., 2006, Phys. Lett. B, 640, 74
Epstein R. I., Baym G., 1988, ApJ, 328, 680
Epstein R. I., Baym G., 1992, ApJ, 387, 276
Epstein R. I., Link B., 2000, in Cheng L. S., Chau H. F., Chan K. L., Leung K. C., eds, Stellar Astrophysics. Kluwer, Dordrecht, p. 95
Espinoza C. M., Lyne A. G., Stappers B. W., Kramer M., 2011, MNRAS, 414, 1679
Flanagan C. S., 1996, in Johnston S., Walker M. A., Bailes M., eds, ASP Conf. Ser. Vol. 105, 'Pulsars: Problems & Progress'. Astron. Soc. Pac., San Francisco, p. 103
Franco L. M., Link B., Epstein R. I., 2000, ApJ, 543, 987
Glampedakis K., Andersson N., 2009, Phys. Rev. Lett., 102, 141101
Grill F., 2011, PhD thesis, Univ. Milan
Gusakov M. E., Kantor E. M., Haensel P., 2008, Phys. Rev. C, 79, 055806
Gusakov M. E., Kantor E. M., Haensel P., 2009, Phys. Rev. C, 80, 015803
Hobbs G., Archibald A., Arzoumanian Z., Backer D., 2010, Classical Quantum Gravity, 27, 084013
Jahan-Miri M., 2005, New Astron., 11, 157
Jahan-Miri M., 2006, ApJ, 650, 326
Jones P. B., 1990, MNRAS, 243, 257
Jones P. B., 1992, MNRAS, 257, 501
Jones P. B., 1993, MNRAS, 263, 619
Jones P. B., 1997, Phys. Rev. Letters, 79, 792
Jones P. B., 1998a, Phys. Rev. Lett., 81, 4560
Jones P. B., 1998b, MNRAS, 296, 217
Jones P. B., 2006, MNRAS, 371, 1327
Larson M. B., Link B., 2002, MNRAS, 333, 613
Link B., 2003, Phys. Rev. Lett., 91, 101101
Link B., 2009, Phys. Rev. Lett., 102, 131101
Link B., Epstein R. I., 1991, ApJ, 373, 592
Link B., Epstein R. I., 1996, ApJ, 457, 844

Link B., Epstein R. I., Baym G., 1992, ApJ, 403, 285
Link B., Epstein R. I., Baym G., 1993, ApJ, 403, 2
Lyne A., Hobbs G., Kramer M., Stairs I., Stapper B., 2010, Sci, 329, 408
Melatos A., Peralta C., 2007, ApJ, 662, L99
Melatos A., Warszawski L., 2009, ApJ, 700, 1524
Melatos A., Peralta C., Wyithe J. S. B., 2008, ApJ, 672, 1103
Middleditch J., Marshall F. E., Wang Q. D., Gotthelf E. V., Zhang W., 2006, ApJ, 625, 1531
Negele J. N., Vautherin D., 1973, Nuclear Phys. A, 207, 298
Pines D., Shaham J., Alpar M. A., Anderson P. W., 1980, Progress Theor. Phys. Suppl., 69, 376
Pizzochero P. M., 2011, ApJ, 743, L20
Pizzochero P. M., Viverit L., Broglia R. A., 1997, Phys. Rev. Lett., 79, 3347
Prix R., Comer G. L., Andersson N., 2002, A&A, 381, 178
Reisenegger A., Goldreich G., 1992, ApJ, 395, 240
Ruderman M., 1975, ApJ, 203, 213
Ruderman M., 1991, ApJ, 382, 587
Ruderman M. A., Sutherland P. G., 1973, ApJ, 190, 137
Ruderman M., Zhu T., Chen K., 1998, ApJ, 492, 267
Schwarz K. W., 1984, Phys. Rev. B, 31, 5782
Sedrakian A. D., 1995, MNRAS, 277, 225
Sedrakian A., 2005, Phys. Rev. D, 71, 083003
Sedrakian A. D., Cordes J. M., 1999, MNRAS, 307, 365
Seveso S., 2010, Master thesis, Univ. Milan
Sidery T., Alpar M. A., 2009, MNRAS, 400, 1859
Sidery T., Passamonti A., Andersson N., 2010, MNRAS, 405, 1061
Smits R., Kramer M., Stappers B., Lorimer D. R., Cordes J., Faulkner A., 2009, A&A, 493, 1161
Sonin E. B., 1987, Rev. Modern Phys., 59, 87
Stappers B. W. et al., 2011, A&A, 530, A80
van Eysden C. A., Melatos A., 2010, MNRAS, 409, 1253
Warszawski L., Melatos A., 2008, MNRAS, 390, 175
Warszawski L., Melatos A., 2011, MNRAS, 415, 1611

This paper has been typeset from a TEX/LATEX file prepared by the author.